

****TITLE****

ASP Conference Series, Vol. ****VOLUME****, ****PUBLICATION YEAR****

****EDITORS****

Inhomogeneous Metallicities and Cluster Cooling Flows

R. Glenn Morris and Andrew C. Fabian

Institute of Astronomy, Madingley Road, Cambridge CB3 0HA, UK.

Abstract. The theme of this contribution is the idea that the metals in the intracluster medium (ICM) may be inhomogeneously distributed on small scales. We focus on the possible interplay between this and the cooling flow process. We begin with a brief review of some evidence for a patchy distribution of metals in the ICM. Next we outline a simple numerical model for this within the framework of the cooling flow hypothesis. Finally we present some of our recent results on the presence of gradients in the observed abundance profiles.

1. Introduction

1.1. The Intracluster Metallicity

It has been known for some time that the mean metallicity of the intracluster medium (ICM) is about 0.3 solar (hereinafter Z_{\odot}); both for nearby (Edge & Stewart 1991), and distant (Mushotzky & Loewenstein 1997) clusters. It is probably fair to say that there is no *a priori* reason why the ICM should be uniformly enriched to this value; for example, if we just consider the relative mass in gas and stars today, which can be $\sim 5:1$.

In addition, simple calculations show that the diffusion time of ions in the ICM is extremely long. For example, Ezawa et al. (1997) estimate that iron can only diffuse ~ 10 kpc or so in a Hubble time. Of course, other effects such as convection, mergers, etc. will act to smooth out the metal profile. These are complicated issues, but it does not seem unreasonable to adopt as a working hypothesis the idea that the metal distribution might not be homogeneous and see what the consequences might be.

Several recent X-ray images of clusters appear to show “cold-fronts” where the surface brightness changes abruptly; for example, the Markevitch et al. (2000) image of A2142. This was used by Ettori & Fabian (2000) to show that thermal conduction must be reduced by a factor of 250–2500 compared to the “classical” value. Here we will only add the comment that if thermal conduction is suppressed, then ion movement will be even more so, since for significant thermal conduction to take place individual electrons do not actually have to travel that far.

Analysis of the *Chandra* image of 4C+55.16 (a powerful radio source in a cooling flow cluster at $z = 0.24$) by Iwasawa et al. (in preparation) shows an extremely high abundance (super-solar) within the central 50 kpc, dropping to around $0.5 Z_{\odot}$ outside this radius.

It is important to stress that these are *not* the kind of inhomogeneity we will consider in the rest of this contribution. We wish to explore the idea that the ICM metal distribution might vary on *small*, essentially unresolved scales. The previous two points are merely evidence that: (i) regions of very different properties can co-exist in the ICM at essentially sharp boundaries; and (ii) regions of extremely high metallicity may exist in the ICM.

1.2. Cooling Flows

Recent observations with the *XMM-Newton* RGS show a discrepancy with the predictions of the standard cooling flow model, with an absence of some of the expected lines from low-temperature species. Various possible explanations have been suggested for this apparent conflict: heating; mixing; differential absorption; metallicity variations; etc. It was for this reason that we first began to consider the last of these, namely small-scale metallicity variations, but from this starting point our investigations have subsequently developed along different lines.

2. The Model

2.1. System Specification and Evolution

We assume spherical symmetry so that the system can be described by a one-dimensional model. A cluster is modelled as a two-component system comprised of hot gas in the potential well of a dark matter halo. The latter is represented by a standard NFW profile. In order to create a realistic cluster mass profile, we make use of the calibrated virial scaling relations of Evrard, Metzler, & Navarro (1996), and take a concentration parameter of 5 as typical of the cluster regime.

To date, the gas has been modelled only as a single-phase medium, i.e. only one temperature and density at any given radius. For initial conditions we assume a hydrostatic pressure profile of the isothermal form. The outer boundary pressure is adjusted so that the gas mass is some appropriate fraction (≈ 0.2) of the total mass.

The gas is allowed to evolve under the effects of gravity and radiative energy loss, using a constant-pressure outer-boundary condition. The 1D hydrodynamics equations are discretised using the Lagrangian method of Thomas (1988). Put simply, the radial range is divided into a large number of zones which are then evolved forwards in discrete time-steps, using an adaptive step-size to maintain stability.

2.2. Metallicity

The radiation from the gas is modelled using the MEKAL spectral code. Consequently, the metallicity is a relevant parameter. Each radial zone may have a different set of abundances for the 15 elements included in MEKAL. Initially, we integrate spectra to build up a discrete evaluation of the cooling function. This is strongly dependent upon the metallicity, with different species controlling the cooling in different temperature regimes. At high ($\gtrsim 10^8$ K) temperatures, the cooling is dominated by the H, He continuum; whereas at lower tempera-

tures line cooling from heavy elements dominates (mainly iron in the 10^6 – 10^7 K regime, with oxygen significant at lower temperatures).

The cooling function may itself be integrated in order to obtain a value for the cooling time. In practice, we only follow the gas cooling down as far as 10^5 K. At such temperatures, the cooling time is becoming prohibitively short for continued computation. Furthermore, the gas has left the X-ray regime and may therefore be neglected (for our purposes). In practice, if any zone falls below 10^5 K we remove it from subsequent calculations and allow the remainder of the gas to adiabatically expand to fill the space (a crude representation of the rapid collapse of cold gas into condensed objects of negligible volume).

2.3. Spectra

At given times during the evolution of the system, X-ray spectra are produced. In order to facilitate comparison with observations, we first integrate along a cylindrical line of sight through the cluster at a given projected radius, to calculate a quantity that may be referred to as the “spectral surface brightness”. Integrating again over a range of projected radii leads to the spectrum due to an annulus. The spectra are then redshifted in terms of energy and scaled according to the luminosity distance. Data are converted to *XSPEC* table-model format FITS files. Simulated observations may then be produced, by convolving the model spectra with the response function of a particular detector (we make use of the *Chandra* ACIS-S proposal-planning response files). The effects of an absorbing column N_H are added by multiplying the model spectra with an *XSPEC* `phabs` model.

3. Results

To investigate the effects of an inhomogeneous metal distribution, we have begun by considering one of the simplest possible inhomogeneities: 9 out of every 10 radial zones are made to be a pure H, He plasma; whilst the tenth zone has a $5 Z_\odot$ abundance of metals. This is clearly a very simple parameterization, but we are concerned not with making detailed predictions, but rather with seeing what the general trends of behaviour might be. In this section we illustrate some of the results for a cluster with the following properties: virial temperature 8.6 keV; gas fraction 0.17; $z = 0.017$; $N_H = 10^{21} \text{ cm}^{-2}$; simulated observation time 25 ks.

Figure 1 shows the results of fitting the fake observations (in the range 0.3–7 keV) for each annulus at various times in the evolution of the system, using a single temperature `mekal` model (multiplied by a `phabs` component). We fix N_H and z at the correct values and allow the temperature, abundance and normalization of the `mekal` component to vary freely.

3.1. Abundance Gradients

Note firstly that the initial conditions are fit as a uniform abundance profile, despite the strong variations in metallicity that are actually present on small scales. This is since in the coronal equilibrium approximation the ions radiate in exactly the same way whether they are concentrated in a particular region or uniformly dispersed throughout the emitting volume. Thus observationally

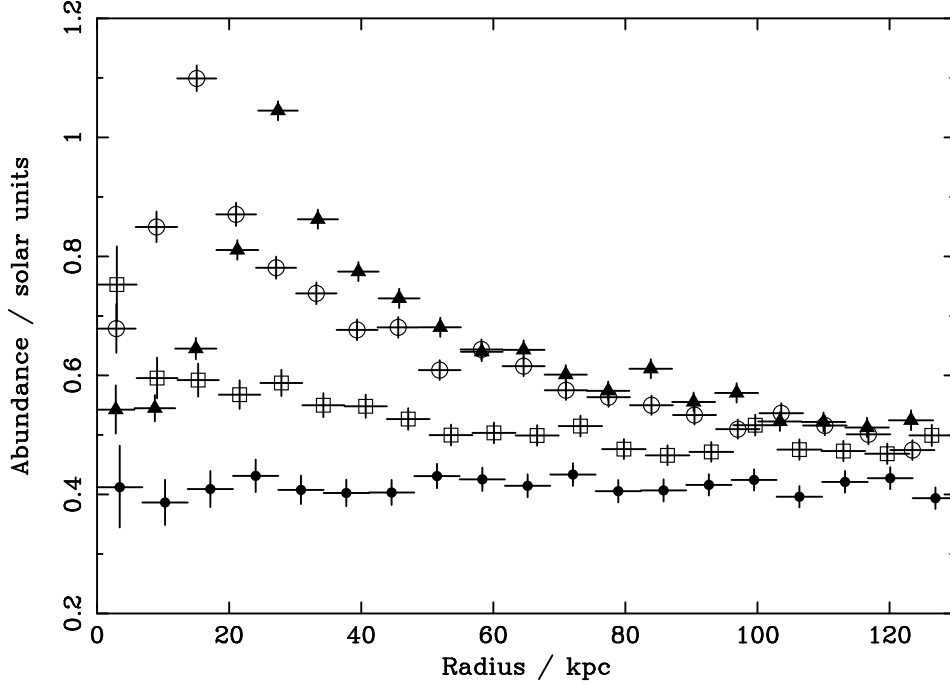


Figure 1. Time evolution of the abundance profile for a bimodal distribution of metallicities. Filled circles - 0.0 Gyr; open squares - 0.6; open circles - 0.9; filled triangles 1.0. Vertical error bars are 1σ .

any fluctuations in abundance that occur on small spatial scales may be very difficult to detect.

As the system evolves, more interesting effects are produced. Initially, there is a rise in abundance in the central regions, leading to the appearance of an abundance gradient in the cluster. As further time passes, the abundance in the very centre of the cluster begins to drop, so that an abundance peak is produced at an off-centre position. The peak works outwards with time. It is important to stress that in these simulations, the actual abundance of the modelled ICM is not time-dependent, but remains fixed. A control simulation with a homogeneous distribution of metals shows no such effects - the abundance profile remains flat.

The apparent rise in abundance in the central regions may be explained as follows. The bulk of the continuum radiation in these models is supplied by the metal-poor gas; whereas all the line emission is due to the metal-rich gas. This has a significantly shorter cooling time than the metal-poor gas owing to its enhanced radiation at all temperatures. The metal-poor gas therefore cools relatively slowly, and consequently we can regard the strength of the continuum as being fairly constant. The high abundance zones on the other hand cool much more rapidly, and as they do so they enter the temperature regime where line emission is even more significant in the cooling function. The net result is that the strength of the emission lines relative to the continuum increases with time, due to the differential cooling rates of the gas contributing to these two components. Recall that it is precisely from the strength of emission lines compared to the continuum (i.e. the equivalent width) that abundances are determined.

Thus the behaviour outlined above is fit as an increase in abundance. The effects are obviously greatest in the central regions where the density is highest and the two-body bremsstrahlung process is most intense. The drop in the central abundance at late times occurs as metal-rich gas cools out and is lost from the X-ray wave-band.

This is an interesting result, because abundance gradients of this form have been detected in several clusters, for example with *ASCA* in Centaurus (Allen & Fabian 1994) and AWM 7 (Ezawa et al. 1997). The presence of a gradient appears to be correlated with the presence of a cooling flow (e.g., De Grandi & Molendi 2001).

Recent *Chandra* observations of Centaurus (Sanders & Fabian, in preparation) and A2199 (Johnstone et al., in preparation) seem to show abundance profiles very similar to those produced here, with a gradient in the outer regions, an off-centre peak and a central abundance drop. In both the models and the data, the effects persist when two-temperature fits are used (as they are in the inner regions when statistically required). It is necessary to tie the abundances of the two components since there is not enough information in the spectra to constrain them separately.

3.2. Equivalent Width Effects

The *ASCA* gradients were seen clearly in the equivalent width of the iron K line. For the model spectra, however, excluding the iron L complex by fitting only in the range 3–7 keV produces different results. In this case, whilst the abundance does rise initially in the central regions, the large off-centre peak seen in Figure 1 never develops. Instead, the abundance merely dies away in the inner regions at later times. Excluding the iron K lines by fitting only to the spectral region 0.3–5 keV produces results very similar to those obtained using the full range.

The discordancy between these two spectral features is caused by the different temperature dependences of their equivalent widths, as illustrated in Figure 2 (calculated from MEKAL spectra). Starting from high temperatures, the equivalent width of the iron L complex increases strongly and monotonically with cooling. The K width on the other hand increases only slightly, then falls off at lower temperatures. Thus when the bimodal metallicity gas is allowed to cool, the strength of the L complex relative to the continuum increases strongly, leading to pronounced rises in the observed central abundance. The relative change in the iron K lines is much less, so fitting exclusively to these spectral features produces less of an effect. Thus small-scale variations cannot produce the observed iron K gradients (but they are not inconsistent with the presence of such gradients — Morris & Fabian, in preparation).

The equivalent widths of the silicon and oxygen K lines are also depicted in Figure 2. Both show a monotonic increase on cooling, but the magnitude of the effect is smaller for oxygen. Using the *vmekal* model in *XSPEC*, we may obtain separate abundance profiles for these elements. Silicon shows a very similar profile to iron, but for oxygen whilst the overall shape is the same, the peak abundance is significantly lower. Thus, this is one way to produce an underabundance of oxygen (but only in the central regions of the ICM, and only with an accompanying gradient).

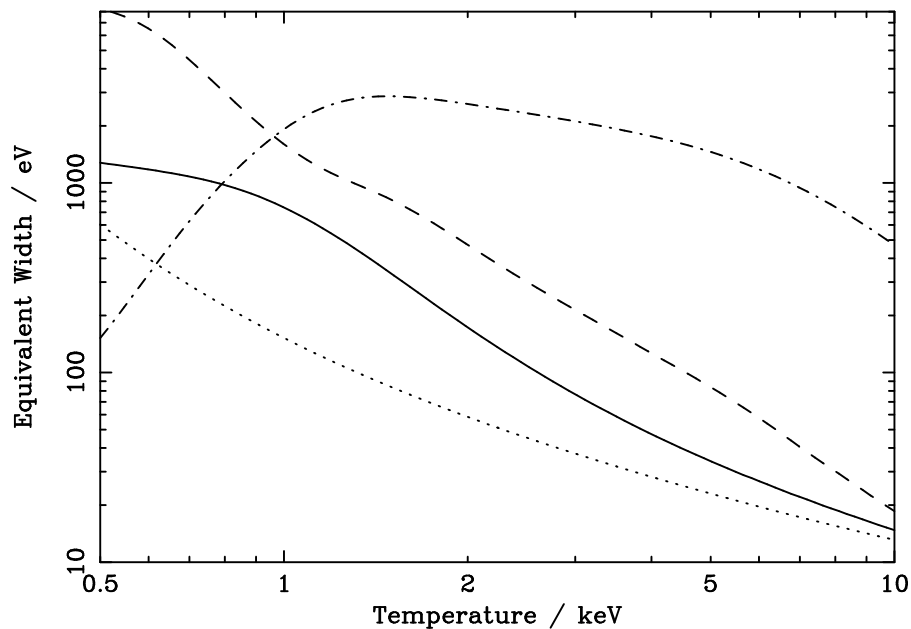


Figure 2. Temperature dependence of some equivalent widths. Dot-dashed iron K; dashed iron L; dotted oxygen K; solid silicon K.

4. Summary

There is reason to think the metals in the ICM may not be smoothly distributed. If this is the case, the cooling flow model predicts a reduced flux of lines from low-temperature species, together with the appearance of (artificial) abundance gradients in certain spectral lines, coupled with a central drop in abundance. All these effects are seen in data (although of course other explanations exist). The persistence of an abundance drop in the centre of the ICM implies limits for the amount of convection and mixing in these regions.

References

- Allen, S. W., & Fabian, A. C. 1994, MNRAS, 269, 409
 De Grandi, S., & Molendi, S. 2001, ApJ, 551, 153
 Edge, A. C., & Stewart, G. C. 1991, MNRAS, 252, 414
 Ettori, S., & Fabian, A. C. 2000, MNRAS, 317, L57
 Evrard, A. E., Metzler, C. A., & Navarro, J. F. 1996, ApJ, 469, 494
 Ezawa, H., Fukazawa, Y., Makishima, K., Ohashi, T., Takahara, F., Xu, H., & Yamasaki, N. 1997, ApJ, 490, L33
 Markevitch, M. et al. 2000, ApJ, 541, 542
 Mushotzky, R. F., & Loewenstein, M. 1997, ApJ, 481, L63
 Thomas, P. A. 1988, MNRAS, 235, 315